The Phase-1 Upgrade of the ATLAS Level-1 Calorimeter Trigger

Niklas Schmitt on behalf of the ATLAS collaboration

***Abstract*—The ATLAS level-1 calorimeter trigger is a custom-built hardware system that identifies events containing calorimeter-based physics objects, including electrons, photons, taus, jets, and total and missing transverse energy. In Run 3, L1Calo has been upgraded to process higher granularity input data. The new trigger comprises several FPGA-based feature extractor modules, which process the new digital information from the calorimeters and execute more sophisticated trigger algorithms. The design of the system will be presented along with an analysis of the improved performance for identifying interesting proton-proton collisions in the increasingly challenging Run-3 LHC pile-up environment.**

***Index Terms*—LHC, ATLAS, FPGA, Level-1 Calorimeter Trigger, Phase-1 Upgrade**

I. Introduction

During the Run 3 data taking period, the Large Hadron Collider (LHC) at CERN was operating with a center of mass energy of 13.6 TeV and about twice the number of simultaneous collisions per bunch crossing (pile-up) compared to Run 2 (see figure 1). As a consequence of the increased instantaneous luminosity and the more challenging data taking conditions, the ATLAS detector [1] and in particular the trigger and data acquisition (TDAQ) system underwent a major upgrade to ensure a successful physics program. An important part of this so-called phase-1 upgrade includes new hardware for the Level-1 calorimeter trigger, which was installed during the LHC *Long Shutdown 2* and commissioned in 2022. It is introduced as a first step towards preparing ATLAS for the transition of the collider towards the *High Luminosity* (HL) LHC, which will increase data rates and pile-up even further.

II. The ATLAS Trigger and Data Acquisition System in Run 3

The ATLAS TDAQ system is an automatic event selection system that is designed to reduce the event rate from the LHC bunch crossing frequency of 40 MHz down to an operationally manageable level by selecting the most interesting events. It is a two staged system, consisting of the *Level-1* trigger and a *High Level Trigger* (HLT). The former maintains a rate of accepted events below 100 kHz, limited by the readout capabilities of the detector. Given the huge data rates and challenging latency requirements it consists of several custom-built, FPGA

Submitted on 29.06.2026

Niklas Schmitt is with the Institut für Physik, Johannes Gutenberg-Universität, Staudingerweg 7, 55128 Mainz, Germany
E-mail: niklas.schmitt@cern.ch.

Copyright 2026 CERN for the benefit of the ATLAS Collaboration. CC-BY-4.0 license

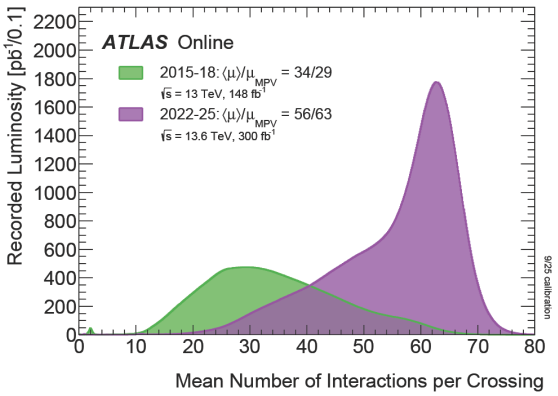

Fig. 1. Luminosity weighted distribution of the mean number of interactions per bunch crossing for LHC Run 2 (2015-2018) and Run 3 (2022-2025) [2].

based hardware modules, performing fast and efficient algorithms within a fixed latency budget of 2.5 μs (including time for data transmission). Three systems of **F**eature **EX**tractors (FEXes) were introduced to identify several physics signatures based on energy information from the calorimeters. With upgraded readout electronics for phase-1, energy information is provided at a finer granularity, compared to the old (Run 2) system. This allows for the implementation of more powerful algorithms improving the efficiency of identifying physics objects, as well as rejecting background.

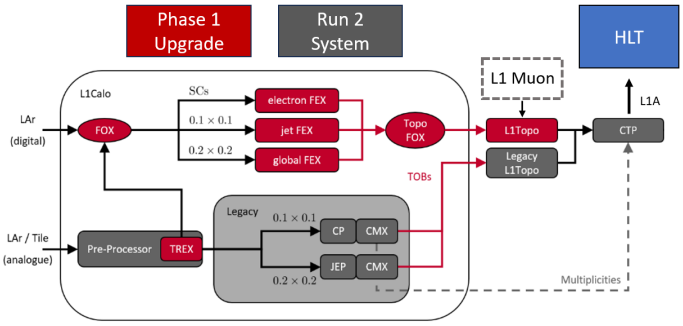

Fig. 2. Overview over the level-1 calorimeter trigger system in Run 3 highlighting the upgrades compared to the old system (adapted from [3]).

Events accepted by Level-1 are buffered, while the HLT aplies more sophisticated algorithms at full detector resolution. The HLT is running software based algorithms on a farm of $\sim 60k$ CPU cores. To reduce processing time, those algorithms are restricted to the area of interest identified at level-1. In the end, the accepted event rate is ~ 3 kHz of data which is read out and stored for physics analysis. Figure 2

gives a detailed overview about the ATLAS level-1 trigger system.

III. Level-1 Calorimeter Trigger

ATLAS operates with two different types of calorimeter systems. The *tile-calorimeter* consists of scintillating tiles and covers the central part of the detector ($|\eta| < 1.6$). It is designed to measure hadronic energies. In addition, the full detector range ($|\eta| < 4.9$) is covered by a Liquid Argon (LAr) based system, measuring hadronic energies in the outer part, as well as electromagnetic energies across the whole coverage. Signals from the calorimeters are available comparatively fast after a collision and are therefore used as inputs for the level-1 calorimeter trigger. Before the upgrade, analog signals were summed to build so-called *trigger towers* representing the energy in an area of $\Delta\eta \times \Delta\phi = 0.1 \times 0.1$ in the central part and even larger windows in the forward region of the detector. For Run 3, upgraded readout electronics on the LAr calorimeter, allows for digitization of the signals on-detector and thus providing information at a finer granularity by subdividing trigger towers in smaller parts, so-called *super cells*. In particular, as illustrated in figure 3, depth information is available, i.e. information for different layers of the calorimeter. The signals are transmitted via optical fibres to the FEXes with a line rate of 11.2 Gbps per link, providing a 3D grid of energy information as basis to run the algorithms for object identification. Digitization for inputs from the tile-calorimeter will be added as part of a future upgrade.

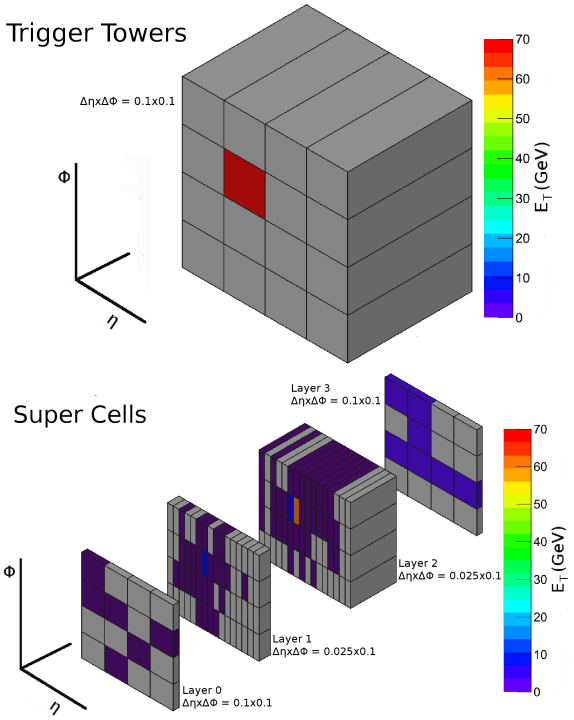

Fig. 3. Energy deposits from a 70 GeV electron in the old system (top) and upgraded trigger electronics for phase-1 (bottom) [4].

L1Calo Feature Extractors

The three FEX systems are designed to identify different kinds of physics signatures and objects of interest. Generally, the design of the modules reflects a trade-off between high granularity information from the calorimeters for a good energy resolution on one hand and a larger area of coverage per module on the other hand. For all FEXes individual FPGAs cover a fixed region within the detector, denoted as algorithmic core region. In addition, duplicated information of data from neighbouring FPGAs is received to mitigate edge effects. Table I summarizes the technical features of the three subsystems. The algorithmic latency budget for the FEXes is 8 bunch crossings (200 ns).

TABLE I
Summary of the key aspects and technical details for each FEX sub-system (based on [1], [5]).

	eFEX	jFEX	gFEX
granularity	0.025×0.1	0.1×0.1	0.2×0.2
coverage	central detector	full detector	full detector
trigger objects	e/γ, τ_{had}	$e/\gamma_{\lvert\eta\rvert>2.5}$, τ_{had} jets, E_T^{miss}, $\sum E_T$	large jets, ρ E_T^{miss}, $\sum E_T$
main FPGAs	XC7VX550T $\times 96$	XCVU9P $\times 24$	XCVU9P $\times 3$
#LUT/FPGA	346k	1 182k	1 182k
input bw/board	~ 1.4 Tbps ($\times 24$)	~ 2.2 Tbps ($\times 6$)	~ 3.4 Tbps ($\times 1$)

Electromagnetic Feature Extractor: The electromagnetic (EM) feature extractor (eFEX) system is designed to identify electrons, photons and tau leptons. It consists of 24 boards (one shown in figure 4), with 4 processor FPGAs per module and receives the input energies with the highest granularity (0.025×0.1) out of all FEXes. Accordingly, it is designed to identify narrow signatures with high precision in the central part of the detector ($|\eta| < 2.5$). The eFEX modules allow for a correction of reconstructed energies to compensate for losses due to *dead material*, i.e. non-active material inside the detector such as cables and support structures.

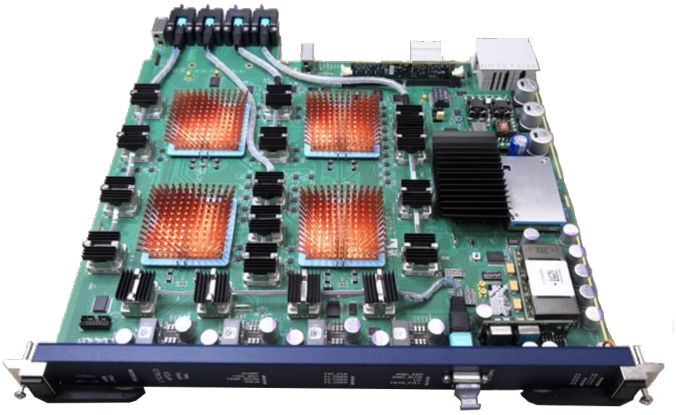

Fig. 4. Photograph of a eFEX production module.

As a result, an improved performance is achieved in finding and triggering on EM objects, as well as rejecting background such as misidentified signatures. Figure 5 shows the efficiency of a single electron trigger as a function of the

electron transverse momentum, comparing the old and the new system. The efficiency curve as seen from eFEX turns-on significantly sharper and in particular in the area before reaching the plateau, more efficient isolation requirements overcome the slow slope visible for the old system. Moreover, the new trigger runs at a $\sim 20\%$ lower rate, highlighting that on top of increasing the signal efficiency, less background is selected.

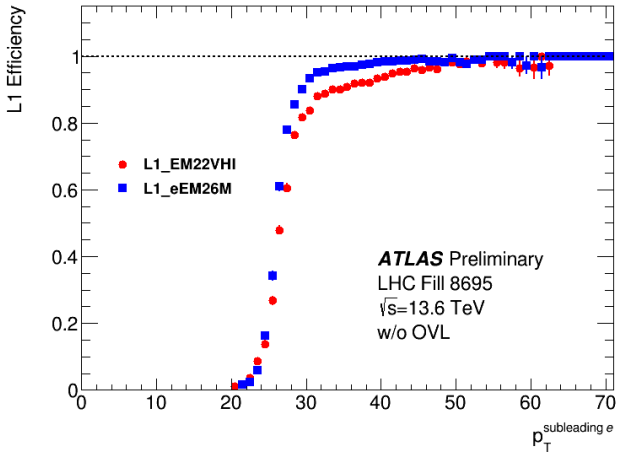

Fig. 5. Comparison of single electron trigger efficiencies between the old (red) and the phase-1 (blue) systems as a function of the transverse momentum of the electrons [6].

Jet Feature Extractor: The jet feature extractor (jFEX) system covers a wide spectrum of signatures. It consists of 6 modules with 4 processor FPGAs, each, and is designed to reconstruct taus, jets, total- and missing transverse energy, covering the whole detector with moderate input granularity of (0.1×0.1). For input treatment, the jFEX system does not only allow for the application of minimum energy thresholds (noise cuts) to reduce electronics noise, but also introduces a dynamic pile-up correction algorithm. The latter corrects the E_T values by subtracting the average energy depositions in the calorimeters originating from pile-up, i.e. underlying energy from simultaneous collisions in the detector. In particular, for algorithms that reconstruct energy sums such as E_T^{miss}, where the vectorial sum of the total energy in the detector is computed, the per-event correction enables more precise energy measurements and hence improved trigger efficiencies. A photograph of a jFEX module is shown in figure 6. Moreover, a finer granularity of inputs allows for a better discrimination of nearby objects on the jFEX. Figure 7 shows that the old system suffered from a systematic loss in efficiency, because in some cases close-by jets were reconstructed as one single highly energetic jet. Therefore, the trigger efficiency never reached the full 100%. The jFEX system overcame this limitation, almost fully recovering the loss in performance.

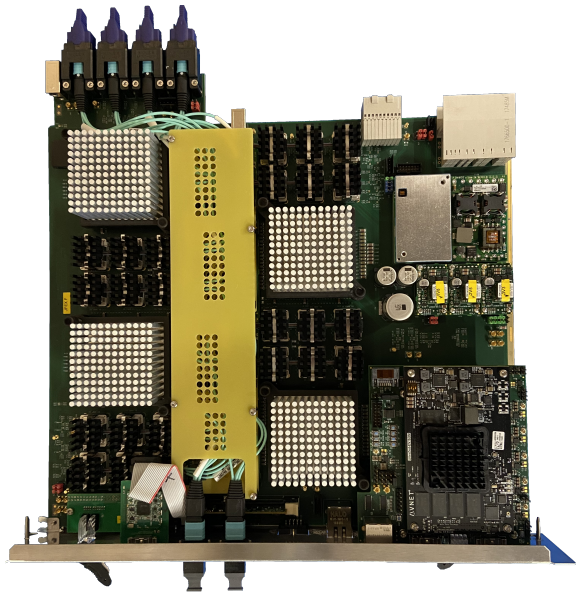

Fig. 6. Photograph of a jFEX production module.

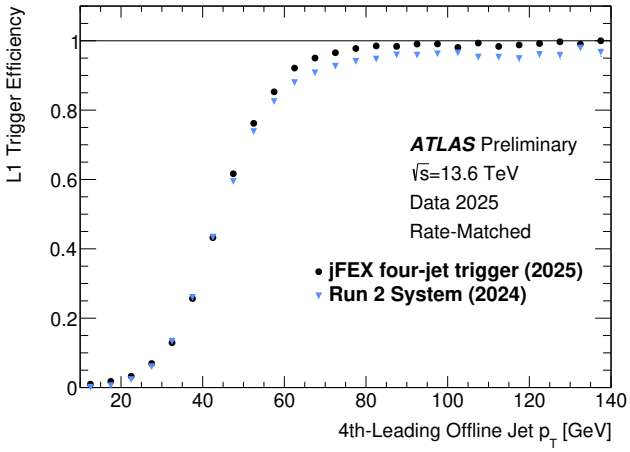

Fig. 7. Comparison of trigger efficiency for a four jet trigger on jFEX (black) and the old system (blue) as a function of the transverse momentum of the fourth-leading jet [6]. The phase-1 thresholds are tuned to result in the same trigger rate as the corresponding item from the old system.

In addition, jFEX acts as a complement to the eFEX system in the forward area where the detector geometry changes, introducing a new algorithm to reconstruct electrons and photons at $|\eta| > 2.3$. The old system did not have a dedicated algorithm for electrons in the forward region of the detector. Because of the poor granularity, electrons were indistinguishable from jets and since the background for jets, especially at small energies, is large, high thresholds were needed to control the trigger rate, limiting the efficiency as illustrated in figure 8. The jFEX system introduced *EM*

Fraction and *EM Isolation* requirements for discrimination against background. Accordingly, the rate-matched jFEX efficiency curve, turns on notably earlier.

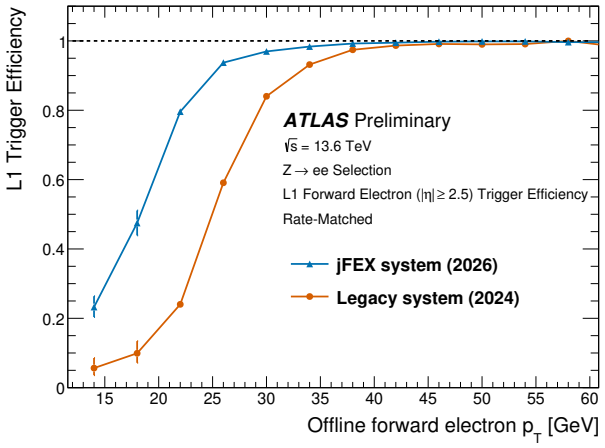

Fig. 8. Comparison of trigger efficiency for forward electrons with $|\eta| > 2.5$ on jFEX (blue) and the old system (orange) as a function of the transverse momentum of the electron [6]. The phase-1 thresholds are tuned to result in the same trigger rate as the corresponding item from the old system.

Global Feature Extractor: The global feature extractor (gFEX) system is composed of one board (shown in figure 9) with 3 processor FPGAs and 1 Zynq FPGA and therefore is designed to collect information from the entire calorimeter with a input granularity of 0.2×0.2 all on one board. It introduces algorithms for estimating the average energy ρ in the detector, as well as suppressing pile-up. The primary purpose of gFEX is the identification of global features, in particular the identification for large-radius jets, where exemplary trigger efficiencies are show in Figure 10.

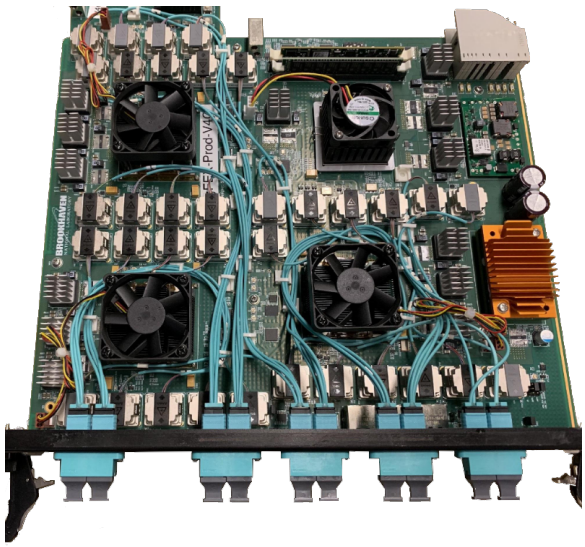

Fig. 9. Photograph of a gFEX production module.

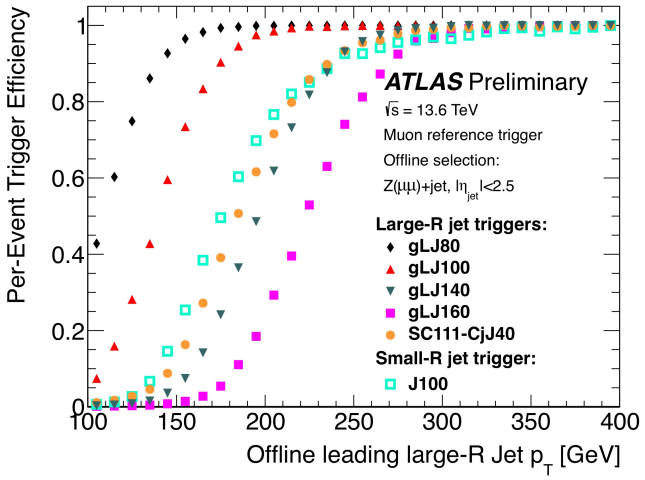

Fig. 10. Comparison of several large-radius jet trigger efficiencies on gFEX with a single jet trigger from the old system (cyan) as a function of the transverse momentum of the large-radius jet [6].

Additionally, gFEX adds complementary algorithms to jFEX for reconstructing missing transverse energy, illustrated in figure 11. While both FEXes outperform the old system, it should be noted that the level-1 topological processor allows for a combination of the two, improving the combined phase-1 performance even further.

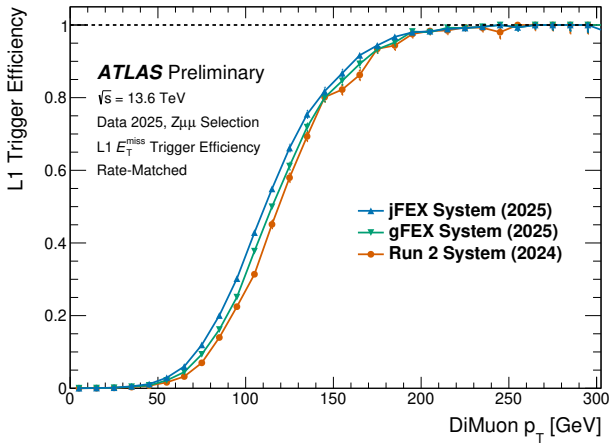

Fig. 11. Comparison of trigger efficiencies for missing energy triggers on gFEX (green), jFEX (blue) and the old system (orange) as a function of the transverse momentum of the invariant mass of the di-muon system, which acts as a proxy for E_T^{miss} in the calorimeters [6]. The phase-1 thresholds are tuned to result in the same trigger rate as the corresponding item from the old system.

IV. Level-1 Topological Processor

The level-1 topological processor (L1Topo) receives all the object candidates from the FEXes, as well as the level-1 muon system. On one hand, it performs multiplicity algorithms that count objects based on different criteria, such as E_T thresholds and isolation requirements also combining information from different subsystems. For example, it matches eFEX tau candidates with the corresponding jFEX objects to form *combined taus*. The latter unites energy information with high

resolution from eFEX and isolation information from jFEX, benefiting from the larger area of coverage. On the other hand, L1Topo reduces trigger rate for example arising from object ambiguities, i.e. cases where the same physical object is reconstructed multiple times by different algorithms. Also topological requirements like angular separations and invariant masses between objects are implemented to exploit distinct physics signatures thus further improving the background rejection. This results in about 200 different decisions that are evaluated by L1Topo. On top of that, it is also designed to increase the efficiency to trigger on a set of special physics events, for instance by correlating information from different bunch crossings (time-slices) thereby improving sensitivity to signatures of long-lived particles. Moreover, small machine learning algorithms can be implemented, such as GELATO[1] [7] a variational auto-encoder for anomaly detection, i.e. identification of event topologies that deviate from standard collision signatures. Therefore, this auto-encoder, which became the first neural network deployed on ATLAS level-1 hardware, can be sensitive to new physics processes, not covered by the standard set of triggers. Figure 12 illustrates the performance of GELATO on various example signal models.

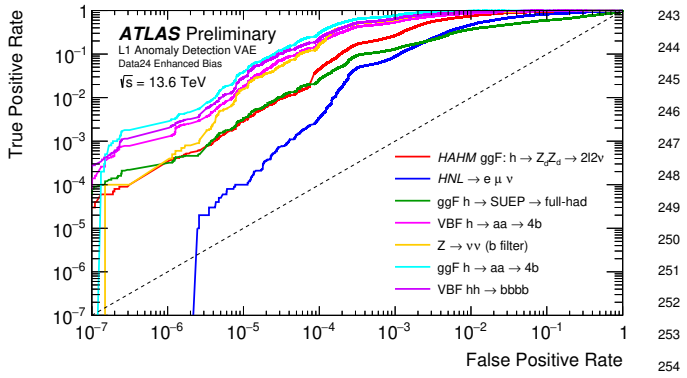

Fig. 12. ROC curves of GELATO for various signal models representing signatures of new physics processes [7].

V. Conclusion

The phase-1 upgrade of the level-1 calorimeter trigger in ATLAS was successfully installed and commissioned in preparation for the Run 3 data taking period at the LHC. Despite the doubling in pile-up, significant improvements in trigger efficiencies across several signatures were achieved. Moreover, the FEXes will remain an essential building block of the future system, alongside more upgrades (phase-2 [8]) that are build in preparation for the HL-LHC period, starting in 2030.

[1]Generic Event Level Anomalous Trigger Option

References

[1] ATLAS Collaboration, "The ATLAS Experiment at the CERN Large Hadron Collider," *JINST*, vol. 3, S08003, 2008. DOI: 10.1088/1748-0221/3/08/S08003.

[2] ATLAS Collaboration. "Website: Luminosity public results run 3." (2025), [Online]. Available: https://twiki.cern.ch/twiki/bin/view/AtlasPublic/LuminosityPublicResultsRun3 (visited on 03/05/2026).

[3] M. Weirich, "Development of new atlas trigger algorithms in search for new physics at the lhc," Ph.D. dissertation, Johannes Gutenberg-Universität Mainz, Mainz, Germany, 2021. DOI: 10.25358/openscience-6407. [Online]. Available: https://openscience.ub.uni-mainz.de/items/c9aa4643-d12d-409c-ab8d-5ea57ff918b6.

[4] ATLAS Collaboration, "ATLAS Liquid Argon Calorimeter Phase-I Upgrade: Technical Design Report," ATLAS-TDR-022; CERN-LHCC-2013-017, 2013. [Online]. Available: https://cds.cern.ch/record/1602230.

[5] ATLAS Collaboration, "The ATLAS trigger system for LHC Run 3 and trigger performance in 2022," *JINST*, vol. 19, P06029, 2024. DOI: 10.1088/1748-0221/19/06/P06029. arXiv: 2401.06630 [hep-ex].

[6] ATLAS Collaboration. "Website: L1calo public plots." (2026), [Online]. Available: https://twiki.cern.ch/twiki/bin/view/AtlasPublic/L1CaloTriggerPublicResults (visited on 02/06/2026).

[7] Sugizaki, Kaito and ATLAS Collaboration, "GELATO: A Generic Event-Level Anomalous Trigger Option for ATLAS in LHC Run 3," CERN, Geneva, Tech. Rep. ATL-DAQ-PROC-2025-020, 2025. [Online]. Available: https://cds.cern.ch/record/2947542.

[8] ATLAS Collaboration, "ATLAS Tile Calorimeter Phase-II Upgrade: Technical Design Report," Tech. Rep. CERN-LHCC-2017-019, 2017. [Online]. Available: https://cds.cern.ch/record/2285583.